Analysis of GNSS data at the Moon for the LuGRE project

(Article begins on next page)

19 April 2024

Analysis of GNSS data at the Moon for the LuGRE project

Alex Minetto
Dept. of Electronics and Telecommunications
Politecnico di Torino
Turin, Italy
alex.minetto@polito.it

Fabio Dovis
Dept. of Electronics and Telecommunications
Politecnico di Torino
Turin, Italy
fabio.dovis@polito.it

Andrea Nardin
Dept. of Electronics and Telecommunications
Politecnico di Torino
Turin, Italy
andrea.nardin@polito.it

Oliviero Vouch
Dept. of Electronics and Telecommunications
Politecnico di Torino
Turin, Italy
oliviero.vouch@polito.it

Gabriele Impresario
Telecommunication and Navigation Unit (UTN)
Agenzia Spaziale Italiana (ASI)
Rome, Italy
gabriele.impresario@asi.it

Mario Musmeci
Telecommunication and Navigation Unit (UTN)
Agenzia Spaziale Italiana (ASI)
Rome, Italy
mario.musmeci@polito.it

Abstract—**The Lunar GNSS Receiver Experiment (LuGRE) aims at testing positioning and navigation at the Moon by using Earth Global Navigation Satellite Systems. Within this framework, to support the scientific mission definition and to process on-ground the data that will be collected, a proper GNSS software receiver is needed, implementing advanced signal processing algorithms that enable it to work in the Moon scenario. This paper discusses the issues and potentialities, presenting the preliminary results of the simulation of the Moon environment, as far as the navigation tasks are concerned.**

Keywords—GNSS, Moon, Space Service Volume, Lunar Missions, Signal Analysis

I. INTRODUCTION

The use of in-orbit Global Navigation Satellite Systems (GNSS) receivers has been experimentally validated within the Space Service Volume (SSV), at Low and Medium Earth Orbits as well as up to Geostationary Earth Orbits [1-6]. Latest missions, then, have unveiled GNSS performance for distances of about 150.000 km away from the Earth's surface. In fact, National Aeronautics and Space Administration (NASA)'s Magnetospheric Multiscale (MMS) mission has demonstrated the use of GPS signals up to this distance. The mission relied on four spacecrafts supplied with high-sensitivity Global Positioning System (GPS) equipment able to provide absolute position information. In its second phase their orbit reached 95,000 miles (152.900 km) from Earth, corresponding to about 41% of the Earth-Moon distance, and the record for the highest altitude fix of a GPS signal has been marked. Additionally, near the Earth, the spacecrafts reached a velocity of 22,000 miles per hour (35,406 km/h), which is the fastest known operational use of a GPS receiver [7][8]. MMS has demonstrated that future space missions can rely on GNSS even at very high altitudes, even though present-day GNSSs were not designed for non-terrestrial use.

On the other hand, cis-lunar and lunar environments are becoming increasingly attractive because their exploitation represents a fundamental step towards the exploration of Mars. In this scenario, it is necessary to have a precise knowledge of the spacecraft location, i.e. orbit determination, and of any elements on the Moon surface or orbiting around it. In the last years, many studies discussed the feasibility of using GNSS receivers at Moon Transfer Orbit (MTO) and lunar orbits. As an example, the authors in [9] analyzed the possibility of using GNSS navigation for Earth-to-Moon missions in the framework of the European Student Moon Orbiter mission. In particular, this study investigated the GPS and Galileo signal availability and the achievable C/N_0 levels, during different phases of the mission, considering an acquisition threshold of 35 dB-Hz. In [10], the design of a GPS L1 C/A receiver, as a proof of concept of navigation system to reach the Moon, is described. The receiver, called WeakHEO, is composed by modules which are specific for the lunar scenario, characterized by high dynamics and low power signal [11]. By processing RF signals generated by a GNSS simulator, it has been verified that this receiver is able to perform acquisition, tracking, data synchronization and demodulation of GPS L1 C/A signals down to 15 dB-Hz. An Orbital Filter (OF) is used to aid the acquisition and tracking stages and to increase the navigation accuracy up to a few hundred meters at the Moon altitude. A technology enhancement of WeakHEO has been done developing the SANAG receiver, which confirmed the possibility of acquiring and tracking (down to 12 dB-Hz) Galileo and BeiDou navigation signals as well. Other studies addressed the use at cis-lunar and lunar environments [12-16].

These studies demonstrated that, thanks to the evolution of the technologies and employing proper algorithmic solutions, it is possible to overcome the obstacles faced by spacecrafts at high altitudes, thus extending the SSV of GNSS use.

The simulation results in [15] show that at the Moon altitude the carrier frequency is affected by a Doppler frequency shift up to 20 kHz and Doppler rate up to 4 Hz/s. Instead, at the beginning of the MTO, the Doppler shift reaches values up to 60 kHz, while the Doppler rate up to 65 Hz/s. Therefore, in order to make the receiver robust against these high dynamics, Doppler shifts and Doppler rates must be compensated. Once the Doppler is compensated, a broader range of techniques can be applied to enhance the sensitivity of the acquisition stage.

In this paper we discuss how, Doppler compensation, high-sensitivity acquisition and tracking techniques can be used in a Moon transit and surface operation scenario. These techniques have been validated on simulated data, through a GNSS software receiver that is the core processing unit of an analysis tool being used to process simulated GNSS signals at the Moon. In fact, this work is being developed within the Lunar GNSS Receiver Experiment (LuGRE), a joint NASA-Italian Space Agency (ASI) payload on the Firefly Blue Ghost Mission 1 (BGM1) with the goal of demonstrating GNSS-based positioning, navigation, and timing (PNT) at the Moon [18]. When launched in 2024, the LuGRE payload will

collect GPS and Galileo measurements in transit between Earth and the Moon, in lunar orbit, and on the lunar surface, and will conduct onboard and ground-based navigation experiments using the collected data. An overview of the mission and of the payload is provided in [18]. As a byproduct, we introduce ongoing work for the design and implementation of the analysis tool that is being used for the definition of the test plan, and later on for the processing of the measurements in the ASI part of the ground segment.

II. LuGRE Scientific experiments

The LuGRE Science Team which is currently encompassing two different teams at NASA and ASI. has identified a set of discrete investigations that together respond to the mission objectives. Each investigation has been associated to a different priority level as P1 (*driving*), P2 (*baseline*), or P3 (*best-effort*), based on its criticality to meet the overall LuGRE science requirements and its relative importance and difficulty. A summary of the driving Science investigations is reported in Table I.

TABLE I.   Driving LuGRE Science Investigations

Objective 1
a) Measure the signal strength throughout the mission and empirically evaluate link budget model.
b) Determine signal availability throughout the mission.
c) Measure Doppler-shift and Doppler-rate profiles throughout the mission.
d) Measure pseudorange from visible satellites during all planned operations periods.
Objective 2
a) Calculate and characterize least-squares multi-GNSS point solutions throughout the mission where a sufficient number of signals are available.
b) Calculate and characterize Kalman filter based navigation solutions onboard throughout the mission.
c) Compare onboard navigation solutions to external sources (e.g., ground-based measurement processing, planned trajectory, Blue Ghost navigation solution).
d) Characterize position, velocity, and time uncertainty and convergence properties throughout mission.
Objective 3
a) Process GNSS observables (e.g., Doppler, pseudorange) with ground-based tools to predict achievable onboard navigation performance.
b) Calibrate ground models with LuGRE data and utilize them to predict achievable navigation performance for future missions.

These investigations will be based on the observation of the data collected by a custom payload designed by the company Qascom, based on the Qascom QN400-Space GNSS receiver. The QN400 is a modular unit in both hardware and software architecture. The receiver is made of two core modules: i) a baseband processor, and ii) a Radio Frequency (RF) front-end. These modules work in tandem to capture RF signals and process them digitally. The receiver utilizes software defined radio (SDR) technologies which provide a high degree of flexibility in allocation of correlation resources and configurable architectures that are customizable to the signals being processed.

The receiver is able to provide i) positioning, velocity and Timing (PVT) solutions, ii) the GNSS *raw observables* obtained during real time operation, as well as iii) snapshots of Intermediate Frequency (IF) digital samples collected by the RF front-end at frequencies L1/E1 and L5/E5, hereafter referred to as *In-phase and Quadrature (IQ) samples*.

These data will be the input for the different science investigations, that require then the development of proper analysis tools being at the core of the mission ground segment. This work also supports the planning of the data acquisition slots within the time windows dedicated to the LuGRE payload during the checkout, transit, and surface phases of the mission. The overall amount of data to be transmitted to the ground-segment will indeed represent a severe bottleneck to the actual availability of the IQ samples. Therefore, quantization depth and sampling frequency must be carefully chosen to let IQ captures coexisting with nominal telemetry and raw observables data. In light of this, the programmable front-end of the QN400 will allow for possible re-configuration through the different mission phases.

III. A software analysis tool for lunar GNSS data

The software analysis tool embeds different processing units able to receive as inputs both the *raw observables* collected by the on-board receiver during normal operation and the *IQ samples* of the GNSS signals. As depicted in Fig. 1, the tool is made of three main parts:

1. A set of advanced Digital Signal Processing (DSP) algorithms that, working on the IQ samples, are in charge of the signal conditioning and quality analysis.
2. A *GNSS software receiver* able to process the IQ samples collected in space throughout a full operational chain (acquisition, tracking, pseudorange construction and navigation solution) for GPS and Galileo in the L1/E1 and L5/E5 frequency bands. This receiver, thanks to a fully software implementation has a high grade of flexibility, thus allowing to configure the parameters of the baseband processing
3. A dedicated *post-processing tool*, fed by the collected raw observables, can perform analysis tasks (e.g. multipath detection) and replicate the on-board navigation solution, or implement advanced navigation algorithms w.r.t. what is implemented in the on-board receiver

The software analysis tool will take advantage also of external sources of information (e.g. precise corrections, or precise ephemeris messages, and assistance data when needed).
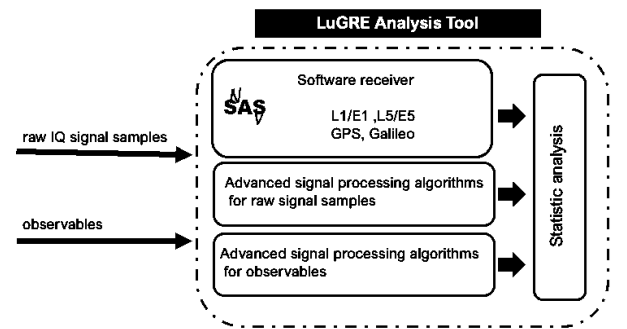

Fig. 1. Block diagram of the software analysis tool for LuGRE

The analysis presented in this paper mostly focuses on the post-processing of the IQ samples that can be handled by hardware or software receivers at the mission ground segment. While limited in duration, these samples can be used to "replay" the lunar signal environment, thus enabling further investigations and characterization. This approach has been already used for critical environments characterized by peculiar features that would be poorly modeled by signal

simulators such as data collected by monitoring stations in remote, Polar regions [19].

IV. SOFTWARE ANALYSIS TOOL DESIGN

The following methodologies are applicable for the pre and post-processing of the IQ samples captured throughout the LuGRE mission. The current study specifically investigate high-sensitivity acquisition and tracking techniques to assess the actual usability of GNSS signals at low Signal-to-Noise Ratio (SNR).

A. Advanced Signal Processing for the IQ samples

The snapshot of IQ samples collected can be processed for signal quality monitoring purposes by means of algorithms that differ from the usual receiver baseband processing. As an example, the analysis tools will implement specific signal conditioning techniques that, with proper compensation can be used for denoising purposes on digital signals. Since thermal noise can be modeled as a zero mean Gaussian random variable, a coherent accumulation process of the samples corresponding to the same code phase in each code period can increase the SNR of the signal up to the point in which the code chips emerge from the noise floor. The digital signal after carrier and data wipe-off, is divided in chunks of length N_{code}, where N_{code} is the number of samples in one code period, as, for example, 1 ms for the GPS L1 C/A signal. L periods contained in the snapshot of IQ signal samples, are coherently summed together, obtaining N_{code} samples that are making visible the shape of the chips of the code. In order to be applied, this technique requires the knowledge of the Doppler shift and Doppler rate profile that have to be compensated for, in order to grant a coherent accumulation of the samples. This technique has been widely used in the past for the blind identification of the codes transmitted by new GNSS satellites [21] or to detect anomalies and evil waveforms [22][23] and it is used in the framework of the LuGRE project to analyze potential distortions due to multipath or other effects.

B. High-sensitivity signal acquisition

In harsh environments, as it is space, the GNSS signal is often subjected to more severe attenuation, leading to lower C/N_0 values w.r.t. the levels experienced in clear sky and therefore to a degraded quality of the estimated position. In these scenarios, high sensitivity GNSS receivers must be employed. These receivers exploit signal processing techniques that allow to increase the robustness of the receiver at low SNR, especially in the acquisition stage. It is known that the main task of the acquisition stage is to find the maximum value of a Cross Ambiguity Function (CAF), corresponding to the best estimation of the code delay $\bar{\tau}$ and the Doppler shift f_D. In order to find these values, the correlation peak must emerge from the noise floor. The higher and the sharper the peak, the more accurate is the initialization of the tracking stage, leading to better performance of the receiver. However, the noise samples, affect each cell of the Search Space (SS) and alter the acquisition result. Assuming zero mean Additive White Gaussian Noise (AWGN), to limit this effect it is possible to exploit averaging operations. Noise averaging can be obtained by increasing the integration time, which means increasing the number of incoming samples used for the evaluation of the ambiguity function. This averaging can be done before or after taking the CAF envelope, corresponding respectively to *coherent integration* and *non-coherent integration* time extension respectively.

To facilitate the acquisition stage, it is fundamental also the use of GNSS assistance data, such as estimated Doppler

shift and Doppler rate. The following section introduce the main strategies and assistance data that improve the acquisition stage.

C. Assistance data

Assistance information are essential to facilitate and speed up the receiver real-time operations. GNSS space-born receivers could experience high relative dynamics with respect to the GNSS satellites, leading to Doppler frequency and Doppler rate values higher than the ones experienced on the Earth surface. Therefore, in this scenario it is relevant to get some a-priori estimates of these values. Such estimates permit to reduce the frequency dimension of the SS and to extend the integration time in the acquisition stage, allowing for the acquisition of GNSS signals characterized by very low C/N_0 levels.

The extension of the integration time is a fundamental strategy for high-sensitivity signal processing techniques. However, when the integration time is increased, the disruptive effects of the Doppler shift on the processing outcome are more evident. Hence, to properly acquire the signal and tracking it, it is important to obtain preliminary estimates of the Doppler shift and Doppler rate and compensate for them. The estimation errors of these two quantities depend on the orbital propagation accuracy. To correctly perform the acquisition and tracking stages, it is fundamental that the error of these estimations is sufficiently low. The Doppler effect has an impact both on the central frequency and on the code frequency of the signal. The first is identified as *carrier Doppler*, while the latter is the *code Doppler*.

In view of the previous considerations, it is important to show the effects of the carrier and code Doppler on the acquisition stage and the results after compensating it. However, besides the high dynamic, space-borne GNSS receivers at altitudes above the GNSS constellation, are characterized by very weak signals reception as well. Hence, to cope with a low SNR, an integration time of $T_{coh} = 150$ ms was considered. Fig. 2a shows the x-y plane of a 3D CAF, when neither the carrier Doppler rate nor the code Doppler are compensated. In this plot, it is evident the shift of correlation peak, caused by the code-chip slipping. In fact, based on the highest correlation values (light areas) the estimated code delay spans from 1013.79 to 1014.61 chips. This happens because along the increased integration time an extended range of carrier and code Doppler levels affect the signal and consequently the CAF. When instead the compensation of both carrier Doppler rate and code Doppler is implemented, the shift of the code delay is absent, as reported in Fig. 2b, where a well-defined peak can be clearly spotted.
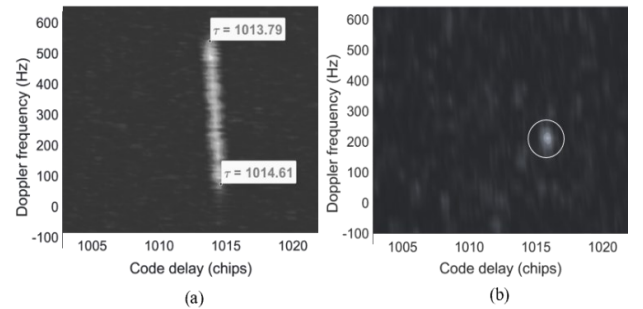

Fig. 2. Acquisition without Doppler compensation (a) and applying both carrier Doppler rate and code Doppler compensations (b), of a GPS L1 C/A code signal having Doppler frequency rate equal to 1800 Hz/s, with $T_{coh} = 150$ ms. Plot of the X-Y plane of the normalized 3-D CAF.

D. High-sensitivity Signal Tracking

The acquisition stage is in charge of initializing the local code replicas at the tracking loop correlators. A stable signal tracking is fundamental to refine the estimation of code delay and Doppler frequency through a Delay Lock Loop (DLL) and Phase Lock Loop (PLL), respectively, whch are the core elements of a GNSS receiver's tracking stage. The DLL and PLL outputs accuracy affect the estimation of pseudorange measurements and condition the demodulation of the navigation message. Besides, an accurate time and frequency synchronization to the received signals, allow for the estimation of the PRN code rate and of the C/N_0. Low C/N_0 values may cause unstable signal tracking, which could result into unwanted phase noise and rotation. Therefore, the demodulation of the navigation message in the investigated scenario is a challanging task and is not foreseen by the actual LuGRE payload. In view of this considerations, an extension of the coherent integration time can be beneficial also when performed within the correlators of the tracking stage. Such an approach can mitigate the effect of a low SNR as long as the Doppler rate conditions are tolerated. The resut is a tradeoff between the sensitivity of the tracking stage and its stability. Therefore an excessive coherent time extension should be carefully avoided.

V. RESULTS

Considering the target scenario, analyses have been carried out to preliminarily assess the performance of a high-sensitivity GNSS software receiver.
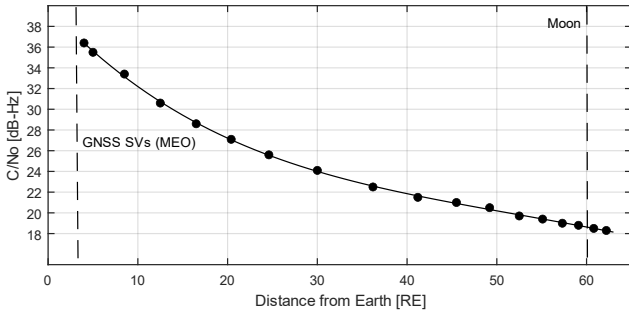
A. GNSS Signal acquisition

Fig. 3. Estimated Link budget along the LuGRE mission trajectory.

Specifically for the acquisition stage, the requirements on the coherent integration time extension have been examined for different C/N_0 levels, consistently with their compatibility with the mission technical bounds. Additionally, by reducing the number of Doppler frequency bins N_D in the acquisition stage, the effect of the system and cell false alarm probability (P_{FA} and P_{fa}) on the overall performance has been investigated. It is assumed that an estimation of the Doppler profile is provided as external aiding, thus a subsequent compensation of the Doppler shift and the Doppler rate, both on the carrier and on the code, is implemented [13].

In view of these considerations, the performance of the acquisition stage, exploiting high sensitivity strategies, has been tested. In particular, coherent and non-coherent accumulation techniques have been utilized. Signals with different C/N_0 have been considered, corresponding to the different distances within the cis-lunar space. To do so, a polynomial model approximating the C/N_0 profile,

depending on the distance from the Earth's centre, has been exploited. Specifically, the addressed scenario focuses on distances greater than those of the MEO orbits of the GNSS satellites. Hence, the model applies to these distances and C/N_0 values concerning distances smaller than the MEO orbits must not be taken into account. Fig. 3 shows the plot of the C/N_0 profile against the distance from Earth, according to the aforementioned model. The MEO region, where GNSS Satellite Vehicles (SVs) are located, is highlighted by a dashed line on the left. While the right, dashed line represents the distance of the Moon from the Earth. As it can be seen from the C/N_0 curve, the higher the distance from the Earth, the lower the C/N_0 values. Actually, what must be considered in this framework is the distance from GNSS SVs, specifically.

However, given the scale of involved distances, referring to the distance from Earth is a reasonable approximation. The worst case scenario is at a distance of about 60 RE, i.e. Earth-Moon distance, where the C/N_0 is expected to reach 18 dB-Hz (worst case), given the characteristics of the hardware and of the antenna expected to be used in the mission.

Table II reports the minimum coherent integration time needed to successfully acquire the signal, for different C/N_0 and limiting the SS to Doppler bins, thus corresponding to different accuracy of the aiding information. In Table II, the minimum duration of T_{coh} to achieve a successful acquisition of the GNSS signals is reported w.r.t. the C/N_0 levels estimated along the trajectory from Earth to Moon (Fig. 3). Each column refers to a different size of the search space, i.e. the number of coherent sums necessary to acquire the signals are reported for each size of N_D and for different C/N_0 levels. By setting a smaller N_D, which means reducing the SS size, the value of T_{coh} necessary to acquire signals is reduced too.

TABLE II. RAW IQ SAMPLE MINIMUM INTEGRATION TIME TO ACQUISRE SIGNALS VERSUS C/NO LEVELS

C/N_0 (dB-Hz)	T_{coh} (ms) (Nd = 3)	T_{coh} (ms) (Nd = 5)	T_{coh} (ms) (Full SS)	T_{coh} (ms) ($P_{fa} = 10^{-8}$)
36.3	4	4	6	4
32.2	6	6	8	6
27.2	45	45	55	45
24.0	90	90	120	90
21.9	100	100	105	100
20.2	160	160	175	160
18.6	230	370	415	230

This is due to the fact that the acquisition threshold is fixed according to statistical rules that depends on the single *cell false alarm probability*, P_{fa}, that is derived from the *system false alarm probability* P_{FA} (related to the entire SS). acquisition outputs have been used to feed the subsequent tracking stage.

B. GNSS Signal Tracking

A subset of scenarios along the mission trajectory has been selected to extend the investigation to the tracking stage while focusing on a limited number of cases for the sake of brevity. An example of successful acquisition was hence assessed for PRN 18 at 30, 45 and 60 RE, as depicted in Fig. 4, and the
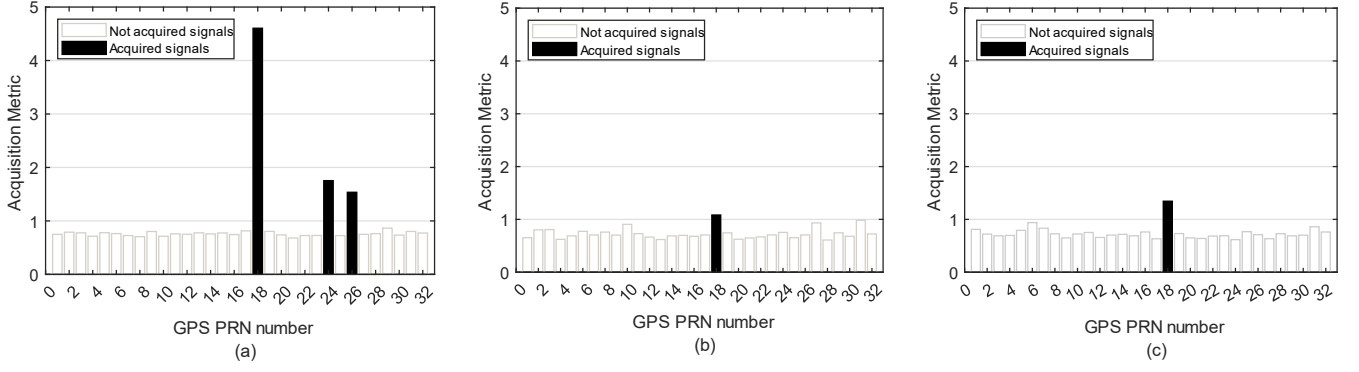
Fig. 4. Examples of acquisition results of GPS L1/CA PRN codes at 30 RE (a), 45 RE (b) and 60 RE (c).
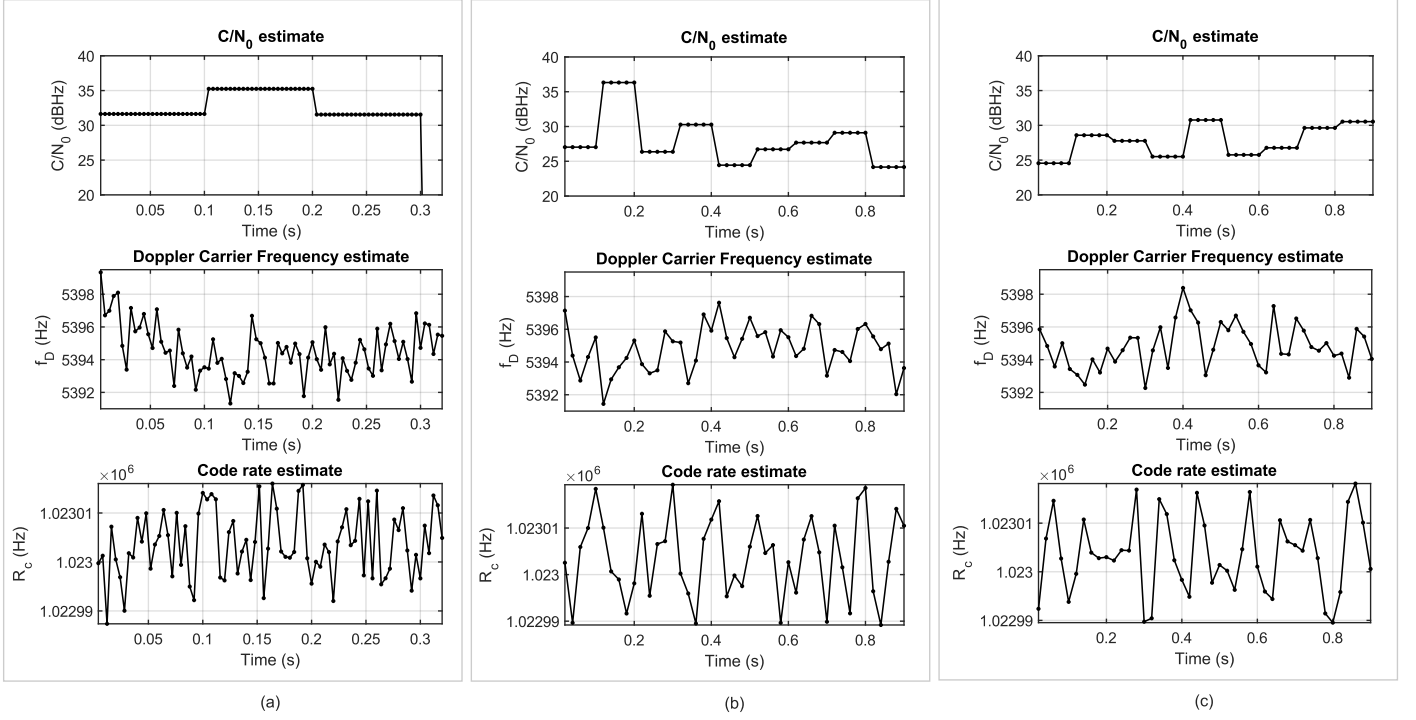

Fig. 5. Examples of tracking results fo GPS L1/CA PRN 18 at 30 RE (a), 45 RE (b) and 60 RE (c).

sample results have been obtained according to the configuration parameters shown in Table III.

TABLE III.   SOFTWARE RECEIVER CONFIGURATION SETTING

Stage	Paramater	Value
Signal Acquisition	Acquisition Coherent Integration Time	10 ms
	Number of Non-coherent accumulations	6
	Doppler bin size	50 Hz
	System False Alarm probability	10^{-3}
Signal Tracking	DLL Bandwidth	10 Hz
	PLL order	3
	PLL Bandwidth	10 Hz
	PLI threshold	0.8
	DLL correlator spacing	1 chip
	Tracking Coherent Integration Time	Variable

By relying on the acquisition parameters and results, the tracking was tested on short signal chunks, to comply with limited time windows dedicated to the downlink for the LuGRE payload. Signal chunks of 300-to-900 ms have been used to assess the feasibility of a signal lock throughout the LuGRE mission phases. The correct lock of the signals has been declared resorting to the Phase Lock Indicator [25]. The three sets of plots in Fig. 5 show the output of the estimated C/N_0 (top), Doppler frequency (middle) and code rate R_c (bottom). The C/N_0 level experienced for each PRN is related to the specific scenario conditions (e.g. visibility of the GNSS satellite). Nonetheless the estimated C/N_0 in Fig. 5 are consistent with the model in Fig. 3. The coherent integration time of the tracking loop correlators has been tuned case-by-case to grant a successful tracking of the signals. At 30 RE, a coherent integration time extension of 4 ms is sufficient to track the strongest GPS signal (PRN 18, see Fig. 4a) as also suggested by the correct estimation of the code rate in Fig. 5a. Moreover, such a limited integration time extension allows to get an acceptable number of tracking loop outputs, processing a very short chunk of signal (300 ms) and thus coping with a limited downlink data rate or data download window. For harsher C/N_0 conditions, such as those experienced at 45 and 60 RE, a larger coherent integration time extension of 20 ms has been employed, leading to the successful lock of PRN 18 also in these cases.

VI. Conclusions

In this paper the analysis tools implemented to support the scientific investigations of the LuGRE project has been introduced. The proposed analysis, performed by simulation, is propedeutic to the definition of the scientific experiments since it is one of the elements to define the length of the IQ sample capture. In fact, such data have a strong impact on the requirements for the on-board storage capacity and have to be compatible with the (limited) data rate and transmission time available during the phases of the LuGRE mission. Despite excluding a pre-processing of the IQ, the results show the sensitivity of the acquisition process to the quality of the Doppler aiding, that have to achieve a proper accuracy to keep the value of N_D small in order to reduce the length of the collected samples.

References

[1] L.M.B. Winternitz, W.A. Bamford, G.W. Heckler, "A GPS receiver for high-altitude satellite navigation", *IEEE J. Sel. Top. Signal Process.* 3(4), 541–556 (2009)

[2] O. Montenbruck, M. Markgraf, M. Garcia, A. Helm, *GPS for microsatellites - status and perspectives". In: Small Satellites for Earth Observation*, ed. by R. Sandau, H.P. Röser, A. Valenzuela (Springer,Heidelberg 2008) pp. 165–174

[3] E. Gill, O. Montenbruck, H. Kayal, The BIRD satellite mission as a milestone toward GPS-based autonomous navigation, *Navigation, Journal of the Institute of Navigation* 48(2), 69–76 (2001)

[4] J. Rush, "Current issues in the use of the global positioning system aboard satellites", *Acta Astronautica*, Volume 47, Issues 2–9, 2000, Pages 377-387

[5] J.R. Vetter: Fifty years of orbit determination: Development of modern astrodynamics methods, John Hopkins APL Tech. Dig. 27(3), pp. 239–252 (2007)

[6] A. Allahvirdi-Zadeh, K. Wang, A. El-Mowafy. *Precise Orbit Determination of LEO Satellites Based on Undifferenced GNSS Observations* Journal of Surveying Engineering, 148 (1), art. no. 03121001 (2022).

[7] National Aeronautics and Space Administration (NASA). *MMS Orbit.* [online].url:
https://www.nasa.gov/mission_pages/mms/spacecraft/orbit.html

[8] M. Farahmand, A. Long, R. Carpenter, Magnetospheric multiscale mission navigation performance using the Goddard enhanced onboard navigation system, *Proc. Int. Symp. Space Flight Dynammics ISSFD*, München ed. by R. Kahle (DLR,Oberpfaffenhofen) pp. 1–17 (2015)

[9] G. Palmerini, M. Sabatini, and G. Perrotta. «En route to the Moon using GNSS signals». In: *Acta Astronautica* 64 (Feb. 2009), pp. 467–483. doi: 10.1016/j.actaastro.2008.07.022

[10] V. Capuano, P. Blunt, C. Botteron, J. Tian, J. Leclère, Y. Wang, F. Basile, and P.-A. Farine. «Standalone GPS L1 C/A receiver for lunar missions». In: *Sensors* 16 (Mar. 2016), p. 347. doi: 10.3390/s16030347

[11] V. Capuano, C. Botteron, J. Leclère, J. Tian, Y. Wang, P-A. Farine, "*Feasibility study of GNSS as navigation system to reach the Moon*", *Acta Astronautica*, Volume 116, Pages 186-201 (2015)

[12] P. Blunt, C. Botteron, V. Capuano, S. Ghamari, M. Rico, and P. A. Farine, "Ultra-high sensitivity state-of-the-art receiver for space applications". In proceedings of ESA Navitec 2016.

[13] V. Capuano, P. Blunt, C. Botteron, P.A. Farine "Orbital filter aiding of a high sensitivity GPS receiver for lunar missions". *Navigation, Journal of the Institute of Navigation*, 64(3), 323-338.

[14] G. Impresario, G. D'Amore, C. Stallo, L. Ansalone, and A. Tuozzi. «GNSS and GALILEO for CIS-Lunar and Moon Navigation». In: *2018 IEEE 4th International Forum on Research and Technology for Society and Industry (RTSI)*. 2018, pp. 1–5. doi: 10.1109/RTSI.2018.8548504

[15] L. Musumeci, F. Dovis, J. Silva, P.F. Silva, and H. Lopes. «Design of a High Sensitivity GNSS receiver for Lunar missions». In: *Advances in Space Research* 57 (Mar. 2016). doi: 10.1016/j.asr.2016.03.020

[16] A. Delépaut, A. Minetto, F. Dovis, F. Melman, P. Giordano, & J. Ventura-Traveset "Enhanced GNSS-based Positioning in space exploiting Inter-Spacecraft Cooperation". In *Proceedings of the 2022 International Technical Meeting of The Institute of Navigation* (pp. 530-544).

[17] Inside GNSS. Italy and Qascom to Land First GNSS Receiver on the Moon. [online]. url: https://insidegnss.com/italy-and-qascom-to-land-first-gnss-receiver-on-the-moon/

[18] J. Parker et al. The Lunar GNSS Receiver Experiment (LuGRE), *Proccedings of the International Technical Meeting 2022 ION ITM 2022*, January 25-27, 2022

[19] N. Linty, F. Dovis, "An Open-Loop Receiver Architecture for Monitoring of Ionospheric Scintillations by Means of GNSS Signals." *Appl.Sci.* 2019, 9, 2482. https://doi.org/10.3390/app9122482

[20] G. Falco, "Dithered sampling and averaging for GNSS signal decoding using conventional hardware". In *Proceedings of the 22nd International Technical Meeting of the Satellite Division of the Institute of Navigation 2009*, ION GNSS 2009, Palm Springs, CA, USA, 22–25 September 2009; Volume 3, pp. 1272–1279.

[21] A. Mitelman, *Signal Quality Monitoring for GPS Augmentation System*. Ph.D. Thesis, Stanford Univeristy, Stanford, CA, USA, 2004.

[22] M. Pini, D.M. Akos, "Exploiting GNSS signal structure to enhance observability".*IEEE Trans. Aerosp. Electron*. Syst. 2007, 43, pp. 1553–1566.

[23] D. Borio, L. Camoriano, and L. Lo Presti. "Impact of GPS acquisition strategy on decision probabilities" In: *IEEE Transactions on Aerospace and Electronic Systems* 44.3 (2008), pp. 996–1011. doi: 10.1109/TAES.2008.4655359

[24] N. Linty, F. Dovis, and L. Alfonsi "Software-defined radio technology for GNSS scintillation analysis: bring Antarctica to the lab", *GPS Solutions*, 22(4), pp. 1-12.

[25] J. J. Spilker Jr., P. Axelrad, B. W. Parkinson, and P. Enge, *Global Positioning System: Theory and Applications*, Volume I. Washington, DC, USA: Amer. Inst. Aeronaut. Astronaut., 1996.